International Journal of Science and Research (IJSR)
ISSN: 2319-7064
SJIF (2022): 7.942

The Influence of Magnetic Flux Rope Events on Galactic Cosmic Ray Anisotropy

G. Adagba[1], B. A. Ikyo[2]

[1,2] Department of Physics, Faculty of Science, Benue State University, Makurdi, 102119, Nigeria

Abstract: ***Galactic cosmic ray anisotropy inferred from ground-based observations during Forbush decrease events can provide very useful information on the local plasma and magnetic field structures such as the magnetic field structures of an interplanetary coronal mass ejection (ICME). This is because galactic cosmic ray distribution allows remote sensing of distant conditions*. Here, we studied GCR anisotropy for two (2) flux rope events; February 2011 and March 2013 events with an aim to compare anisotropy features of the two events. *Our results showed that for both events; FD of February 2011 and FD of April 2013 at times with strong magnetic fluctuations and strong cosmic-ray scattering, there were spikes of high perpendicular anisotropy and weak parallel anisotropy. These results, along with the near constancy of parallel anisotropy across magnetic field reversals, are consistent with diffusive barriers causing the decrease in GCR flux before the arrival of the flux rope. In contrast, within the CME flux rope there was a strong parallel anisotropy in the direction predicted from a theory of drift motions into one leg of the magnetic flux rope and out the other. This result confirms that FD events associated with flux ropes can influence GCR flux in a similar way.***

Keywords: cosmic rays - Sun: coronal mass ejections (CMEs) - turbulence

1. Introduction

Galactic Cosmic Ray (GCR) flux has been known to decrease with geomagnetic storms, due to the passage of a shock or magnetic flux rope associated with arrival of a coronal mass ejection (CME) [1,2, 3]. This can also cause variations in the distribution of GCR. Consequently, the significance of GCR anisotropy and Forbush decrease cannot be overemphasized. For example, it is well understood in the literature that variations in the anisotropy and flux of galactic cosmic rays due to either the passage of a shock or a magnetic flux rope associated with a coronal mass ejection can provide very important and useful information on the properties of solar wind plasma [1,2, 4,6]. In addition to the above, a good knowledge of galactic cosmic ray anisotropy can provide remote information about the interesting structures of CME flux ropes, and this could be related to various space weather effects and space weather forecasting. GCR anisotropy can also shed light on understanding the propagation of GCR [5].

With aforementioned motivation, there have been comprehensive studies about the characteristics of Forbush decreases and their causes, where the arrival of a CME shock has been identified as the major cause of Forbush decrease [1, 6, 7,8].

The anisotropy of GCRS has also been investigated by several authors. For example, Cane [6], showed that, CMES cause depressions in the cosmic ray intensity both locally, when an observer is inside the interplanetary structure (ejecta) and remotely, if the ejecta is energetic enough to create an interplanetary shock to which the observer is magnetically connected. After the shock and ejecta have passed, the intensity gradually recovers as particles diffuse in around the shock.

Also, in their studies; Tortermpun et al.[2],developed a technique to determine the Galactic cosmic ray anisotropy during a Forbush decrease using data from worldwide network of neutron monitors for a single where the arrival of a CME shock has been identified as the major cause of Forbush decrease event.

Sequel to the previous studies, we have modeled GCR anisotropy for two (2)flux rope events using a technique initially developed by Tortermpun et al. [2] and later modified by Ihongo G.D. et al. [3],alongside normalized count rates from polar NM stations, with an aim to compare GCR anisotropy during these Forbush decreases. The events include Forbush decreases of: 18 February 2011 and 13 April 2013.

Appropriately, the components of the anisotropy vector δ are first determined in GEO coordinates before converting to GSE coordinates. This is to avoid fitting a count rate mismatch unrelated to the anisotropy [2, 3]. The anisotropy vector in GSE is further decomposed into components parallel and perpendicular to the interplanetary magnetic field **B**. This is to enable us interpret the result in the solar wind frame.

Our results showed that for both events; that is FD of February 2011 and FD of April 2013, at times with strong magnetic fluctuations and strong cosmic-ray scattering, there were spikes of high perpendicular anisotropy and weak parallel anisotropy. These results, along with the near constancy of parallel anisotropy across magnetic field reversals, are consistent with diffusive barriers causing the decrease in GCR flux before the arrival of the flux rope. In contrast, within the CME flux rope there was a strong parallel anisotropy in the direction predicted from a theory of drift motions into one leg of the magnetic flux rope and out the other, confirming that the anisotropy can remotely sense a large-scale flow of GCRS through a magnetic flux rope.

2. Data and Method

The procedure used here closely follows that of [2,3]. First, we selected two (2) candidate events for this study. We based our selection on events that have clear plasma and magnetic field structures. The detailed procedure and information on the sources of data are discussed in the following sections.

2.1. Data Information

We used data from polar NM stations with good statistics and no major data gaps during the period of Forbush decrease for all events. These stations and their geographic locations along with their geomagnetic cutoff rigidities are presented in table 1 (modified from [2]) for all events.

The neutron monitor data were obtained from the Neutron Monitor Database[1]. We used data from all available polar stations in this database of the worldwide network of neutron monitors with good data for the time period considered. We also used level 2 data from the ACE spacecraft[2] for the solar wind speed, magnitude (B) and geocentric solar-ecliptic (GSE) components of the interplanetary magnetic field.

Table 1: Sources of Neutron Monitor Data

NM Location	Station Code	Geographic Latitude (deg)	Geographic Longitude P_c (GV)	Cutoff Rigidity P_m (GV)
Thule, Greenland	TH	76.5	-68.7	0
Fort Smith, Canada	FS	60.02	-111.93	0
Peananuck, Canada	PE	54.98	-85.44	0
Barentsburg, Russia	BA	78.06	14.21	0
McMurdo, Antarctica	MC	-77.9	166.6	0
Terre Adelie, Antarctica	TA	-66.55	140	0
Nain, Canada	NA	56.55	-61.68	0.01
South Pole, Antarctica	SP	-90	0	0.09
Inuvik, Canada	IN	68.36	133.72	0.18
Mawson, Antarctica	MA	-67.6	62.87	0.22
Jang Bogo, Antarctica	JB	-74.62	164.23	0.3
Tixie Bay, Russia	TB	71.36	128.54	0.48
Norilsk, Russia	NO	69.26	88.05	0.58
Apatity, Russia	AP	67.57	33.4	0.65
Oulu, Finland	OU	65.05	25.47	0.81
SANAE, Antarctica	SA	-70.32	-2.35	1.06
Kerguelen,near Antarctica	KE	-49.35	70.25	1.14

2.2 Method

The first order anisotropy δ of galactic cosmic rays can be determined from the count rate of NM station *n* at a given time *t*, using the following general equation [2,3]:

$$A_n(t) = \sum_{l=0}^{8} wl \int_{P_{min\,,n\,l}}^{P_{max}} \left(\frac{-dN(P_c)}{dP_c}\middle|P\right) T_{n\,,l}(P)\,\frac{P}{D(t)+P} \times \left\{1 + [\delta_x(t) + \chi_x(t,P)]n_{n,l,z}(t,P) + \left[[\delta_y(t) + \chi_y(t,P)]n_{n,l,z}(t,P)\right] + [\delta_z(t) + \chi_z(t,P)]n_{n,l,z}(t,P)\right\} dP \quad (1)$$

In equation 1, *l* is one of 9 directions with weights *wl*set to 1/2 for the vertical direction and 1/16 for the other 8 directions at zenith angle 30° and azimuthal angles equally spaced over 22°.5 – 337°.5 [13, 2]. N(P_c) is the NM response function, and the Dorman fit from a latitude survey during 2004-2005 was used for this[2,3, 10]. This survey year was selected because it is the survey year for which the modulation of galactic cosmic rays was similar to that of the selected events. The transmission function T_{nl}(P) is set to 1 in this analysis because only polar stations were used. δ_x, δ_y *and* δ_z represent the first order anisotropy in. GEO_x, GEO_y, and GEO_z, -components respectively, and χ is the Compton-Getting anisotropy. Finally, the unit vector $\boldsymbol{n}(t,P)$accounts for the asymptotic directions of GCR at NM stations; to find the asymptotic directions we used a particle trajectory code from the Bartol Research Institute [11,12], together with an accurate model of the terrestrial magnetic field including any field disturbance present as indicated by the K_p, index value at each hour.

To avoid a mis-representation of the fixed North-South anisotropy $(\delta_z(t))$and equatorial anisotropy $(\delta_x(t))$ and $(\delta_y(t))$, we first evaluate $(\delta_z(t))$ in GEO coordinates using the following equation [2, 3]:

$$\frac{T(t)-M(t)}{2P_t\,(t)} = \frac{\sum_{l=0}^{8} wl \int_{P_{min\,,n,l}}^{P_{max}} \left(\frac{-dN\,(P_c)}{dP_c}\middle|P\right) T_{n,l\,(P)} \frac{P}{D(t)+P} [\delta_z(t)+\chi_z(t,P)][n_{T,l,z}(t,P) - n_{M,l,z}]dP}{2\sum_{l=0}^{8} wl \int_{P_{min}}^{P_{max}} \left(\frac{-dN\,(P_c)}{dP_c}\middle|P\right) dP} \quad (2)$$

Where T(t) and M(t) are the normalized count rates of Thule and McMurdo respectively. P_t (t) is the average count rate of all

stations. Here, we have used only polar stations with geometric cutoff rigidity approximately 1 GV and as such the transmission T = 1.

Then we determine the equatorial anisotropy $(\delta_x(t))$ and $(\delta_y(t))$ by performing a least square fit to equation (3)

$$\frac{C_n(t)}{C_{n,d}(t)} = \frac{A_n(t)}{B_n(t)} \quad (3)$$

From (3), $C_n(t)$is the count rate of individual stations at a given time t, $A_n(t)$ represents the modeled count rate, $B_n(t)$ models the daily average over equatorial directions and is equal to $A_n(t)$ but with $n_{n,l,x} = n_{n,l,y} = 0\ and\ C_{n,d}(t)$ is the daily running average defined by equation (4). We calculate this by defining $C'_n(t)$ as the NM count rate $C_n(t)$ divided by the average count rate$P_t(t)$. Then we use equation (4) and multiply the result by $P_t(t)$:

$$C'_n(t) = \frac{1}{2}\left[C'_n(t) + \left(\frac{C'^{-}_n(t) + C'^{+}_n(t)}{2}\right) - \frac{1}{4}\left(\frac{C'^{--}_n(t) + C'^{++}_n(t)}{2} - C'^{-}_n(t)\right)\right] \quad (4)$$

Where $C'^{-}_n(t)$, $C'^{--}_n(t), C'^{+}_n(t)\ and C'^{++}_n(t)$the count rates of same NM are stations at times *t – 12hours*, *t – 24 hours*, *t + 12 hours* and *t + 24 hours* respectively. Then we used$C_{n,d}(t) = C'_{n,d}(t)P_t(t)$. The daily running average as defined in equation (4), is designed to average over any daily wave in the normalized count rates. Then $C_{n,d}(t)$ is modeled using$B_n(t)$.

The anisotropies obtained from the procedure described in section 2 are first converted from GEO coordinates to GSE coordinates and further decomposed into components parallel and perpendicular to the interplanetary magnetic field **B**. This is to enable us interpret the anisotropy results in the solar wind frame. The result for our analyses is presented in section3.

3. Results and Discussion

We have used the method described in section 2 to analyze two (2) candidate flux rope events (events with flux ropes hereafter referred as "flux rope events"). The results for analysis are presented in figures 1-2

3.1 Results

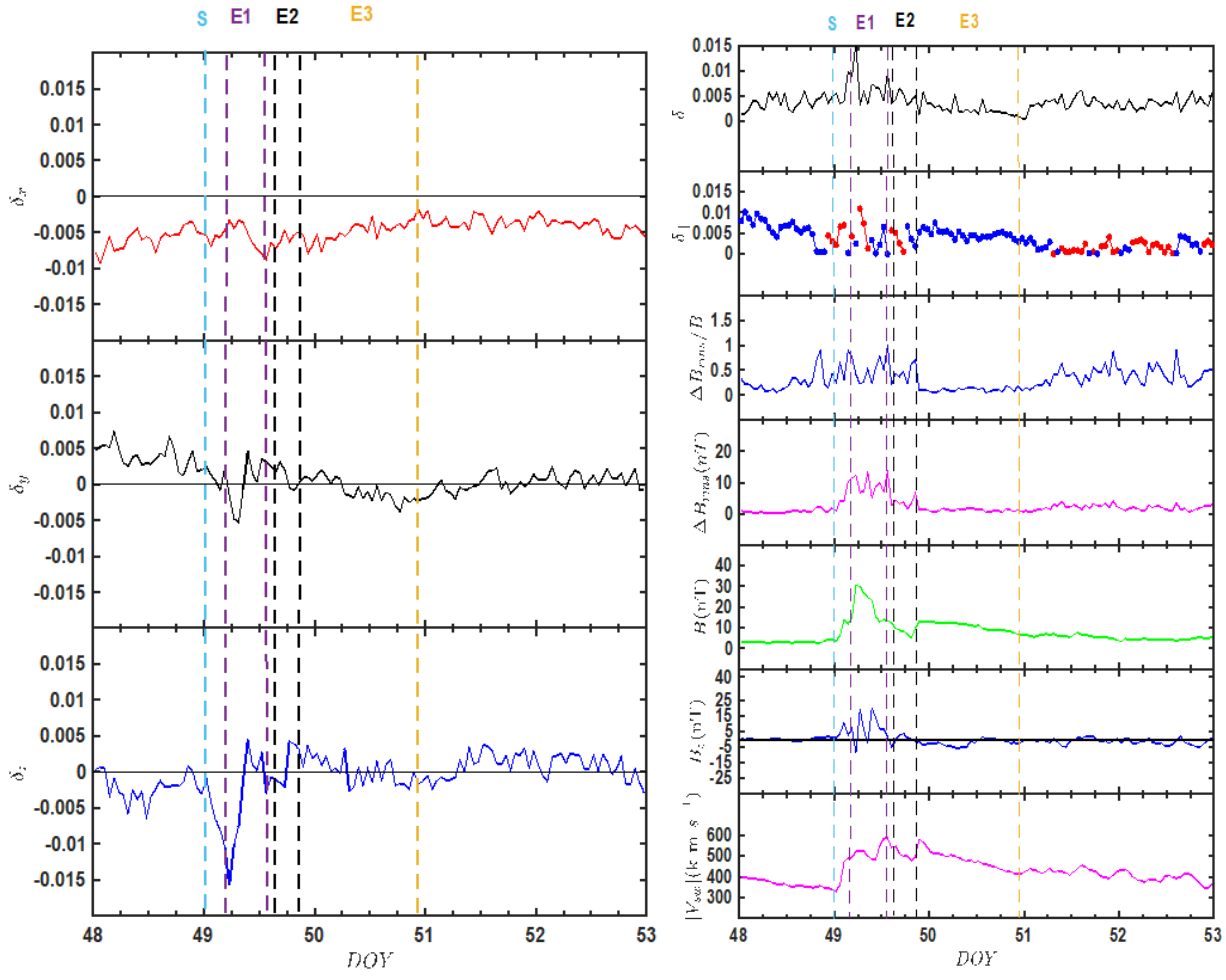

Figure 1a (left): Cosmic-ray 1st-order anisotropy in the solar wind frame for the February 2011 event as derived from polar NMcount rates. Vertical dashed lines indicate event times at Earth.**1b**(right):Cosmic-ray 1st-order anisotropy magnitude in the solar wind frame perpendicular $(\delta_\perp)$ and parallel (δ_{ll}) to theinterplanetary magnetic field (IMF) for theFebruary 2011 as

derived from polar NM count rates, as well as the rms magnetic fluctuation $\frac{\Delta B_{rms}}{B}$ and B_{rms} from ACE /MAG, the IMF magnitude (B) and GSE z-component (Bz) from ACE/MAG, and the solar wind speed (|Vsw|) from Wind/SWE. Vertical dashed lines indicate event times at Earth as in Figure 1a; note that the times are shifted one later in our calculations hence all times are assumed to be at Earth. For δ_{ll}, the color indicates a higher GCR flux when viewing along B (blue) or along -B (red).

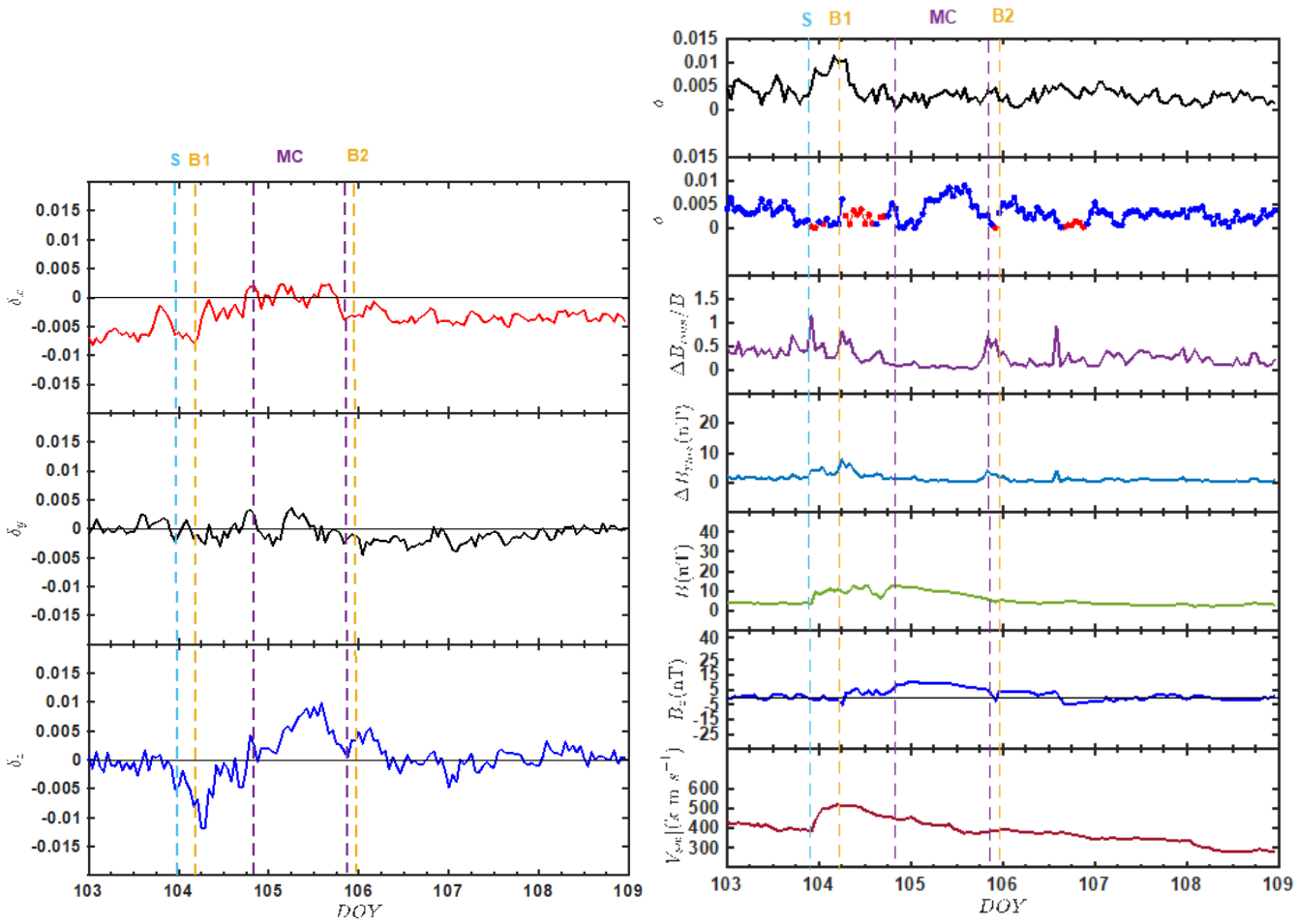

Figure 2a (left): Cosmic-ray 1st-order anisotropy in the solar wind frame for the February 2013 event as derived from polar NMcount rates. Vertical dashed lines indicate event times at Earth.**2b**(right): Cosmic-ray 1st-order anisotropy magnitude in the solar wind frame perpendicular ($\delta_{\perp}$) and parallel (δ_{ll}) to the interplanetary magnetic field (IMF) for the February 2013 as derived from polar NM count rates, as well as the rms magnetic fluctuation $\frac{\Delta B_{rms}}{B}$ and B_{rms} from ACE /MAG, the IMF magnitude (B) and GSE z-component (Bz) from ACE/MAG, and the solar wind speed (|Vsw|) from Wind/SWE. Vertical dashed lines indicate event times at Earth as in Figure 1a; note that the times are shifted one later in our calculations hence all times are assumed to be at Earth. For δ_{ll}, the color indicates a higher GCR flux when viewing along B (blue) or along -B (red).

3.1 Flux Rope Events

The flux rope events in the context of this paper are FD events caused by the arrival of shocks from the following ICMES: ICME of 2011 February 18 and ICME of 2013 April 13-16, which exhibit similar FD patterns in the shock-sheath region. The results of these flux rope events are presented in figures 1 and 2. The first-order anisotropy of GCR can be influenced by many physical processes [2,3], these include but are not limited to the following: Parallel flow, as proposed by [13] within a CME flux rope; perpendicular diffusive anisotropy, due to cosmic ray scattering and diffusion perpendicular to the large-scale magnetic field [2,14]. In particular, Cane et al.[15] proposed that GCRS enter a closed CME flux rope via perpendicular diffusion: parallel diffusive anisotropy, which has been attributed to inhibited parallel diffusion, e.g., a diffusive barrier at the shock [2, 16]: precursory anisotropy before an FD can exhibit unusual pitch angle distributions attributed to parallel scattering effects, perpendicular guiding center drifts and gradient anisotropy due to particle gyration [2, 17].

In order to accurately interpret our results and to determine which effect explains the first-order anisotropy (δ) in the solar wind frame, we resolve δ into components perpendicular and parallel to the magnetic field. The magnitudes of these components, $\delta_{\perp}$ and $\delta_{\parallel}$, respectively, are shown in Figures 1a and 2a respectively.

To begin with, the ICME of 2011 February 18 was associated with three (3) ICMES [18]. The first two did not have a low-variance (low δB) flux rope that crossed the Earth but the third did. We observed a decrease in CR count rates during the first few hours of DOY 49, which occurred

mainly in the sheath region between the shock and the start of the ejecta (E1). As noted by [10, 15], the FD basically had a single step. There was a spike in perpendicular CR anisotropy during hours 4-6 corresponding to a spike in$\frac{\delta B}{B}$, which is consistent with the theory of perpendicular diffusion [7, 15].

In contrast, there was very low parallel CR anisotropy at that time, and also before the shock arrival at about hour 20 of DOY 48. These were times of spikes in$\frac{\delta B}{B}$. This is consistent with quasi-linear theory of parallel diffusion [19], as these should be times with low diffusion coefficient and hence a low parallel CR decrease. Overall, this pattern is consistent with the idea that the CR decrease is due to a diffusive barrier blocking CR flow along B [20].

Also, at times of El and E2, during E1, at hour 6 of DOY 49 when B was near its peak, there was a sharp decrease in δB. This was associated with a spike in parallel anisotropy and a drop in perpendicular anisotropy. These are both consistent with diffusion theory. At the start of E2, at hour 13 of DOY 49, B was low and there was an upward spike in δB, there was a spike in perpendicular anisotropy and a drop in parallel anisotropy, again consistent with diffusion theory.

While time of E3 had a magnetic flux rope with low magnetic fluctuations and a smooth rotation of **B** and highest GCR flux when viewing along$-x_{GSE}$, so observed GCR flow is Sunward. For this case, Shalchi[13],predicted a unidirectional flow associated with cosmic rays entering one leg of the flux rope and exiting the other. To determine the direction of anisotropy predicted by Shalchi [13], we need to see a reconstruction of the field line winding structure in the flux rope. This event was studied by Shalchi [13], and references therein. So, axis of flux rope was basically along$-x_{GSE}$, or outward from Sun. GCR flux was highest when viewing outward. Left-handed flux rope, so when looking to Sun, fields are clockwise and expelling particles. Thus, Shalchi [13] predicted flow from beyond Earth, with inward flow as observed.

The time after E3 is the recovery phase of the FD that is after the flux rope passage, δB increased. Also, parallel anisotropy decreased and perpendicular anisotropy decreased, again consistent with a diffusive anisotropy and consistent with theoretical expectations.

For the 2013 event, we find that there is often an increase in $\delta_{\perp}$at times with stronger rmsfluctuations (ΔB_{rms}). This is consistent with diffusive anisotropy and theories of perpendicular diffusion [2, 3,14], that perpendicular diffusion increases with increasing (ΔB_{rms}/B).

In contrast, $\delta_{\parallel}$ was generally lower during times with stronger magnetic fluctuations and higher during times of weak fluctuations, for instance, within a CME flux rope where magnetic fluctuations are very weak. This is in good agreement with theoretical expectations that strong fluctuations can cause strong cosmic ray scattering leading to low parallel diffusion coefficient [2,3]. This is also consistent with the idea that a parallel diffusive barrier is responsible for the decrease of cosmic ray flux in the sheath region [16]. Note that in Figure 6, we indicate the sign of $\delta_{\parallel}$ in terms of higher GCR flux when viewing along **+B** (blue) or **–B** (red). The color often changes with the reversal of **B**, which is consistent with the idea that parallel scattering and flow processes do not necessarily depend on the sign of **B.**

Within the CME flux rope, there was a strong parallel anisotropy in the direction predicted from the theory of drift motion into one leg of the magnetic flux rope and out the other [13], confirming that the anisotropy can remotely sense a large-scale flow of GCRs through a magnetic flux rope.

References

[1] Forbush, S. E., On the Effects in Cosmic-Ray Intensity Observed During the Recent Magnetic Storm **(**1937), Phys. Rev, 51.
[2] Tortermpun, U., Ruffolo, D., and Bieber, W. J., Galactic Cosmic-Ray Anisotropy During Forbush Decreases: Evidence for Diffusive Barriers and Large-Scale Flow (2018), *ApJL, L26*
[3] Ihongo, G.D., D. Ruffolo, A. Sáiz, U. Tortermpun, J. W. Bieber, and A. C.-L. Chian, Galactic Cosmic-Ray Anisotropy During Forbush Decreases: Evidence for Diffusive Barriers and Large-Scale Flow, *POS (ICRC 2019) 1084.*
[4] Tsurutani, B.T. & Gonzalez, W. D., Handbook of the Solar-Terrestrial Environment (1997), in *Magnetic Storms, Geophys. Monogr. Ser., Vol. 98 pp 355–374*
[5] Amenomori M., Bi, X. J., Chen, L. T. et al. Northern Sky Galactic Cosmic Ray Anisotropy between 10 and 1000TeV with the Tibet Air Shower Array (2017), *ApJ, 836:153 (7pp*)
[6] Cane H. V., Coronal Mass Ejections and Forbush Decreases (2000), *Space Science Reviews, 93*
[7] Lockwood, J. A., Forbush decreases in the cosmic **radiation (**1971), *Space Sci. Revs. 12.*
[8] Barnden, L. R., Causes of Forbush Decreases and Other Cosmic Ray Variations (1973a), *in Proc. 13th Int. Cosmic Ray Conf. 2, 1271.*
[9] Bieber, J. W., Clem, J., and Evenson, P., Cosmic Rays entry from Heliosphere to Variable Magnetosphere K. Kudela, IEP SAS Košice, Slovakia, (1997), *Proc. ICRC (Rome), 2, 389*
[10] Lin Zhongmin, Bieber, J. W., Evenson, P. Electron Trajectories in Model Magnetosphere Simulation and Observation Under Active Condition (1995), *JGR, 100, No A12*
[11] Nuntiyakul, W., Evenson, P., Ruffolo D., Saiz, A., Bieber, J.W., Clem, J., Pyle, R., Duldig, L. M., and Humble. E. J. (2018). Bare Neutron Counter and Neutron Monitor Response to Cosmic Rays During a 1995 Latitude Survey*JGR, 123*
[12] Krittinatham, w., &Ruffolo, d., Drift Orbits of Energetic Particles in an Interplanetary Magnetic Flux Rope (2009), *ApJ, 704, 831.*
[13] Shalchi, A.A. Unified Particle Diffusion Theory for Cross-Field Scattering: Subdiffusion, Recovery of Diffusion, And Diffusion In Three-Dimensional Turbulence (2010), *ApJL, 720, L127*.
[14] Ruffolo, D., Pianpanit, T., Mathaeus, W. H., &Chuychai, P. RANDOM BALLISTIC interpretation

of Nonlinear Guiding Center Theory (2012), *ApJ, 747, L34.*

[15] Cane H. V., Richardson, I.G., &Wibberenz, G. Galactic Cosmic Ray Intensity Response to Interplanetary Coronal Mass Ejections/Magnetic Clouds (1995), *Proc. ICRC (Rome), 4, 377*.

[16] Wibberenz, G., le Roux, J, A., Potgieter, M. S. & Bieber, J, W., Transient Effects and Disturbed Conditions (1998), *SSRv, 83, 309*

[17] Ruffolo, D., Transport and acceleration of energetic charged particles near an Oblique shock (1999),*ApJ, 515, 787*

[18] Vemareddy, P., & Zhang, J., Initiation and Eruption Process of Magnetic Flux Rope from Solar Active Region NOAA 11719 to Earth-Directed CME (2014), *ApJ, 797, 80*

[19] Jokipii, R. J., Comics – Ray Propagation I. Charge Particles in a Random Magnetic Field (1996),*ApJ 146, 480J*

[20] Wibberenz, G., le Roux, J, A., Potgieter, M. S. & Bieber, J, W., Transient Effects and Disturbed Conditions (1998), *SSRv, 83, 309*